Supporting information

Non-crystalline Titanium Oxide Catalysts for Electrochemical Oxygen Reduction Reactions

Satoshi Tominaka,*[,†] Akimitsu Ishihara,*[,‡] Takaaki Nagai[§] and Ken-ichiro Ota[§]

†*International Center for Materials Nanoarchitectonics (MANA), National Institute for Materials Science (NIMS), 1-1 Namiki, Tsukuba, Ibaraki 305-0044, Japan.*

‡*Institute of Advanced Sciences, Yokohama National University, 79-5 Tokiwadai, Hodogaya-ku, Yokohama, Kanagawa 240-8501, Japan*

§*Green Hydrogen Research Center, Yokohama National University, 79-5 Tokiwadai, Hodogaya-ku, Yokohama, Kanagawa 240-8501, Japan*

Contents

1. Additional TEM images

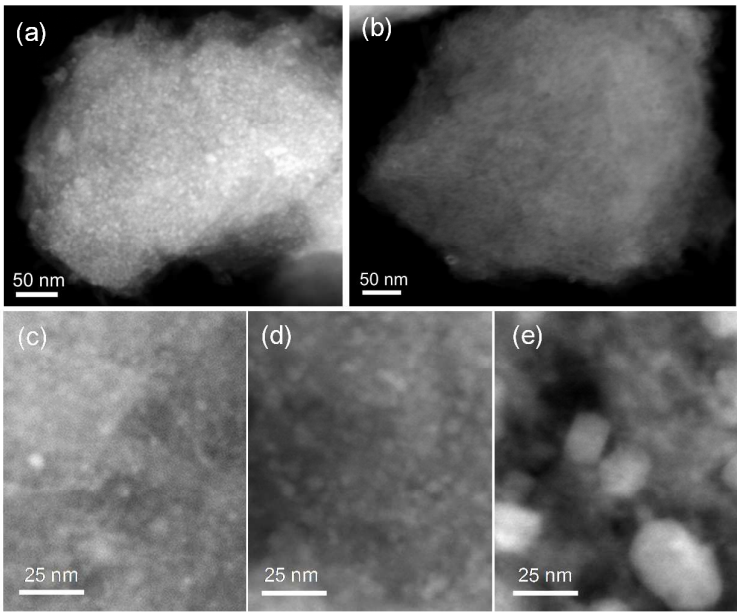

Figure S1. HAADF-STEM images. (a, b) Low-magnification image of the sample annealed for 3 h (a) and the same sample after HF-treatment (b). (c-e) High-magnification images of the samples annealed for 0 h (b), 3 h (c) and 10 h (d).

2. Additional ORR measurement data

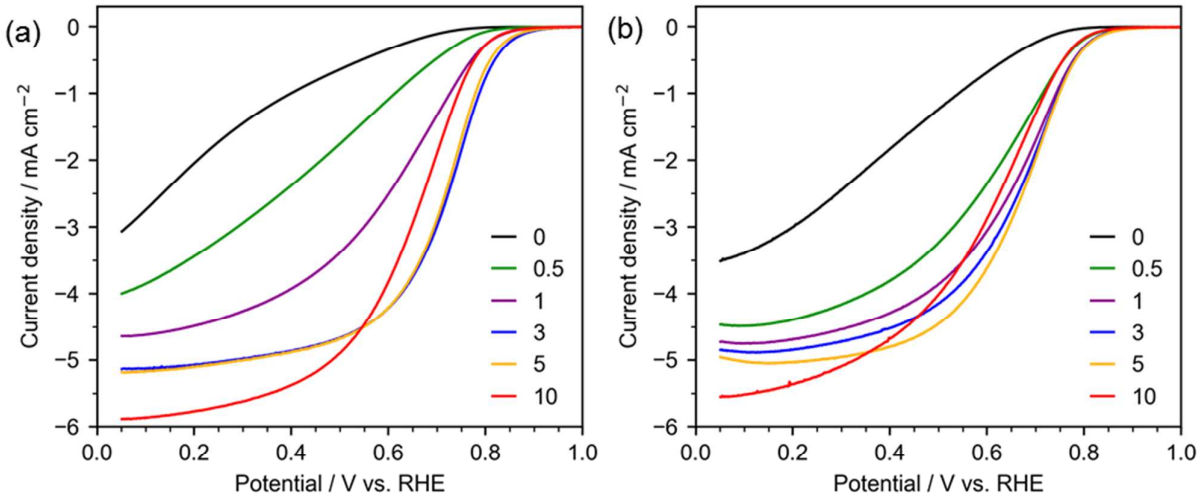

Figure S2 Linear sweep voltammograms of the oxygen reduction reactions on the catalysts annealed for a different period. The samples with (a) and without (b) titanium oxides are compared. The data were collected in 0.1 M H_2SO_4 (negative sweep) after double layer charge corrections. These current densities are based on the geometric areas.

3. Activity associated with carbon materials

One may be interested in the activity associated with the carbon materials only (though they are not focus of our work), hence we summarize our analysis on the carbon materials as follows. The activity associated with carbon materials only cannot be accounted for by the amount of pyridinic N, which should be the active sites in nitrogen-doped carbon materials;[1] because the amount of pyridinic N monotonically decreased with the annealing time as found in XPS (**Figure S4**. Thus, the activity trends of the HF-treated samples shown in **Figure 1c** (red curve) should originate from the change in the size of the π-conjugated system, which should change the activity per site though these changes might not be apparent as the structures appear constant in PDFs (**Figure S5**).

In addition to these, we also compared the activity of the carbon samples prepared by HF-treatment with and without a re-annealing process. **Figure S3** shows that the re-annealing process, which is considered to improve the crystallinity of the carbon phase, did not improve the kinetically controlled current density (or catalyst activity), rather changed resistance or diffusion controlled current.

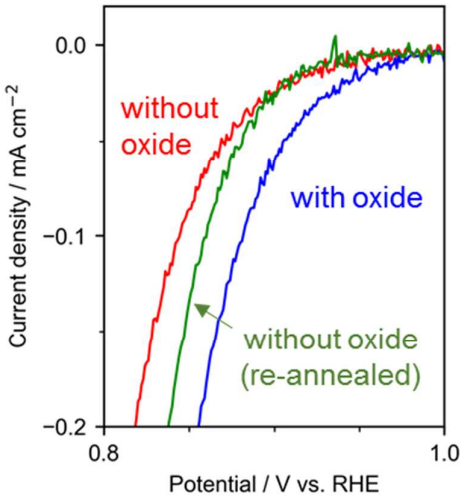

Figure S3 Linear sweep voltammograms of the oxygen reduction reactions on the catalysts annealed for 3 h (blue curve = as-prepared sample; red curve = sample treated with HF; green curve = sample treated with HF and then re-annealed under nitrogen atmosphere for 3 h). The data were collected in 0.1 M H_2SO_4 (negative sweep) after double layer charge corrections. These current densities are based on the geometric areas.

4. Composition analysis using XPS

If electron correlations exist (*i.e.*, Koopmans theorem is not valid), the intensities of the peak associated with the presence of Ti^{III} may not reflect its exact amount,[2-3] but if it is not the case, the compositions are (0 h) $Ti^{IV}_{0.76}Ti^{III}_{0.24}O_{1.6}N_{0.12}$ or $TiO_{1.6}N_{0.12}$; (0.5 h) $Ti^{IV}_{0.78}Ti^{III}_{0.22}O_{1.8}N_{0.16}$ or $TiO_{1.8}N_{0.16}$; (1 h) $Ti^{IV}_{0.89}Ti^{III}_{0.11}O_{2.0}N_{0.05}$ or $TiO_{2.0}N_{0.05}$; (3 h) $Ti^{IV}O_{2.2}N_{0.02}$; (5 h) $Ti^{IV}O_{2.2}$; (10 h) $Ti^{IV}O_{2.3}$.

One may concern the detection depth of the XPS measurements, hence we calculated inelastic mean free path of the photoelectrons as follows. Under our measurement conditions, the inelastic mean free path of photoelectron from Ti 2p state is 1.7 nm through graphite (2.2 g cm^{-3}) and 2.1 nm through rutile TiO_2 (4.27 g cm^{-3}).[4] The detection limits can be twice as deep as these values. Considering the fact that densities of such amorphous carbons in our samples should be one or two order(s) of magnitude lower than dense graphite, we consider that the measurements can detect particles even embedded in carbon (namely, not only ones on the outer surface). Note that the HF treatment did not change the compositions and the relative peak heights except for the removal of the N-species associated with TPPz molecules in the samples annealed at 900°C for 0 h (**Table S4**).

Table S1. Surface compositions (at%)

	Titanium oxide phase				Carbon phase				
	Ti(IV)	Ti(III)	O(Ti-O)[a]	N(Ti-N)	C	O(quinone)[a]	O(COOH/COH)	N(pyridinic)	N(graphitic)
0 h (as)	0.94	0.29	1.3	0.30	86	4.1	2.1	2.4	3.2
0 h (HF treated)	0.15	0.0	0.0	0.0	89	4.1	1.3	1.8	3.3
0.5 h (as)	0.95	0.27	1.5	0.31	88	3.9	2.1	1.4	2.0
0.5 h (HF treated)	0.10	0.0	0.0	0.0	92	3.5	0.98	1.2	2.0
1 h (as)	1.1	0.13	1.9	0.10	88	3.5	2.0	1.2	1.7
1 h (HF treated)	0.06	0.0	0.0	0.0	92	4.0	0.90	1.1	1.8
3 h (as)	1.3	0.0	2.1	0.02	88	5.0	1.3	0.88	1.3
3 h (HF treated)	0.0	0.0	0.0	0.0	93	3.9	0.73	0.71	1.2
5 h (as)	1.3	0.0	2.2	0.0	88	4.8	1.8	0.60	1.1
5 h (HF treated)	0.0	0.0	0.0	0.0	94	4.1	0.56	0.60	1.1
10 h (as)	1.5	0.0	2.3	0.0	90	3.8	1.3	0.47	0.91
10 h (HF treated)	0	0	0.0	0.0	95	3.3	0.34	0.40	1.0

[a] The peak around 531 eV is assignable to carboxylate and hydroxides, while peak around 532 eV assignable to quinone group. Since these peaks are close, the deconvoluted peak areas may contain large errors.

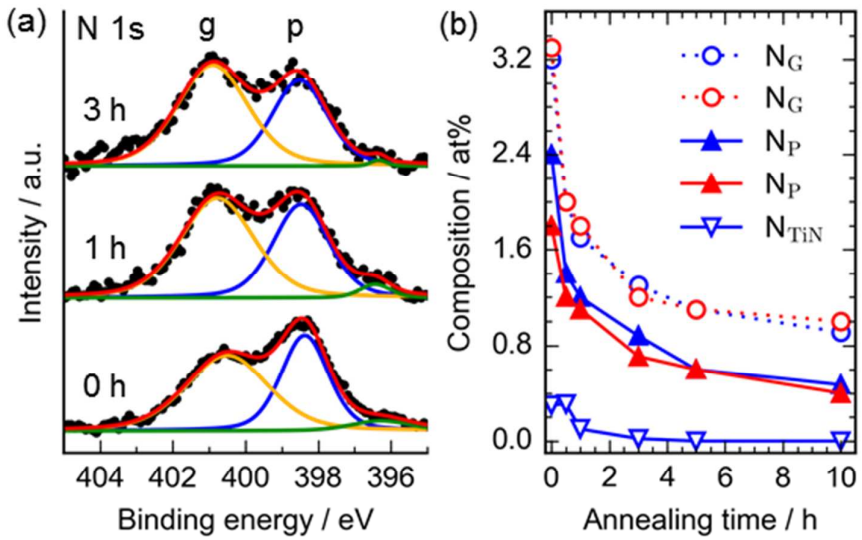

Figure S4 Elemental states of N atoms analyzed by core-level X-ray photoelectron spectra: (a) N 1s spectra. The black dots show the experimental data, the red curves are the simulated spectra, and other curves are fitted peaks of the Voigt functions. (b) Composition changes with annealing time for the samples with (blue) and without (red) titanium oxides.

5. PDF data of carbon materials (HF-treated samples)

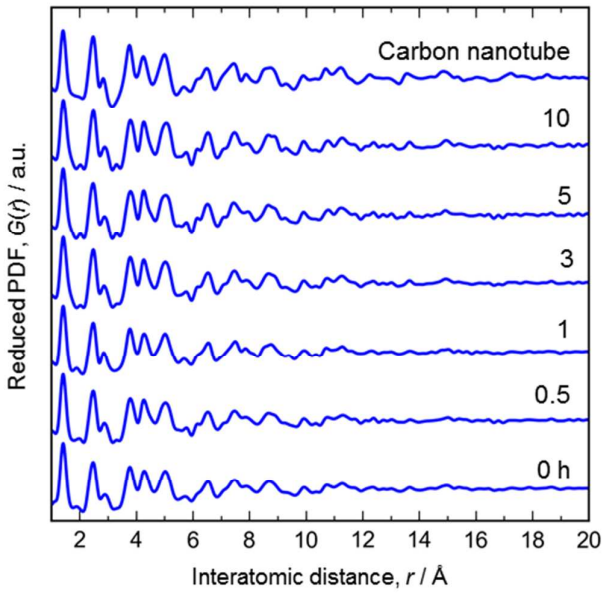

Figure S5 X-ray pair distribution functions of carbons (Q_{max} = 20.0 Å^{-1}). The total scattering data of the carbon nanotubes was subtracted from the total scattering data of the samples treated with hydrofluoric acid, and then the data were converted into PDFs in order to obtain the PDFs of the amorphous carbon only.

6. Additional XPS data

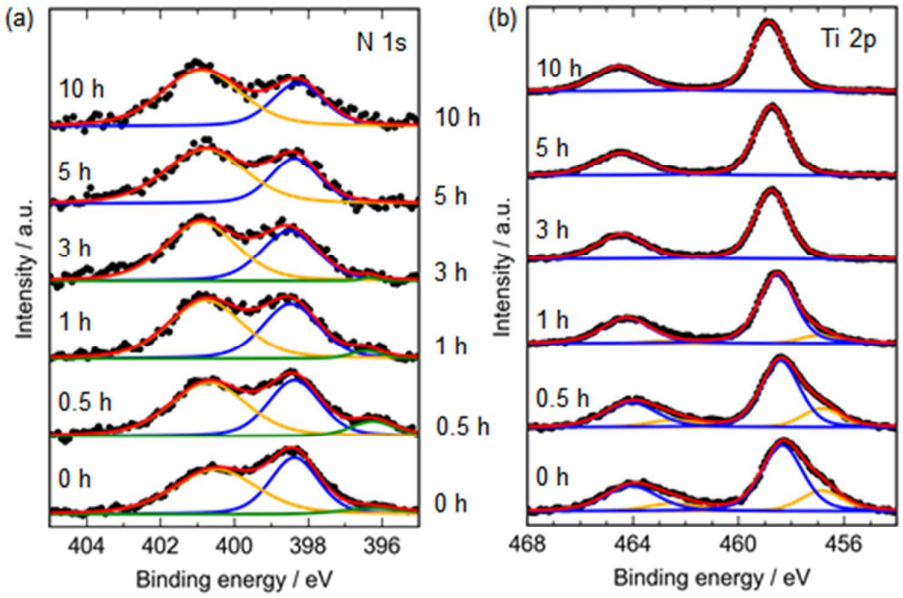

Figure S6 Core-level X-ray photoelectron spectra: (a) N 1s spectra. (b) Ti 2p spectra. The black dots show the experimental data, the red curves are the simulated spectra, and other curves are fitted peaks of the Voigt functions.

7. Additional PDF data

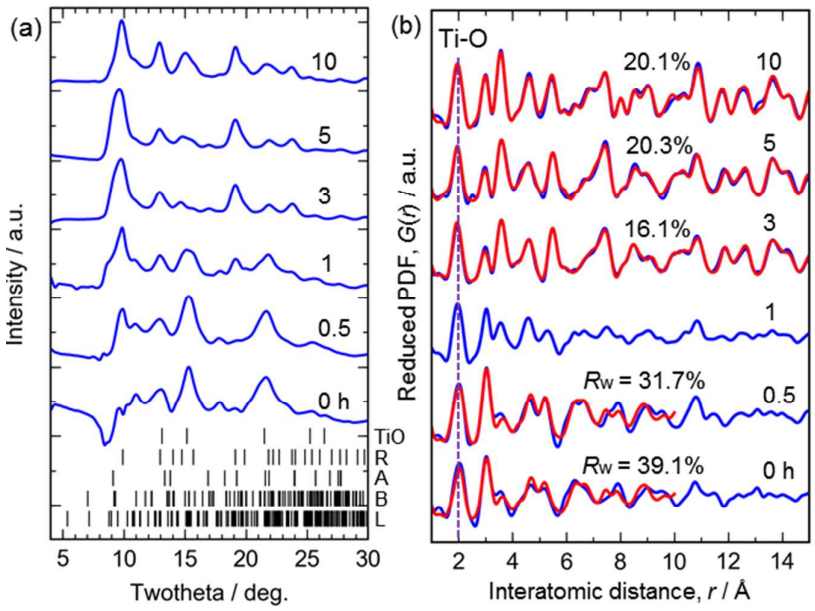

Figure S7 X-ray structure analysis. (a) Total scattering data (λ = 0.556 Å). The data are shown with shifts for clarity. The bottom lines represent Bragg peak positions of TiO, rutile, anatase, brookite and anhydrous lepidocrocite-type TiO_2 (from top to bottom in this order). (b) Pair distribution functions (Q_{max} = 17.5 $Å^{-1}$). The experimental data (blue) were fitted with simulated curves (red) based on structure models: (*i*) lepidocrocite-type TiO_2 (0 and 0.5 h), (*ii*) rutile and brookite (3 h), and (*iii*) rutile, brookite and TiO-type structure (5 and 10 h). The fitting range was 1–10 Å for 0 and 0.5 h, and 1–20 Å for others.

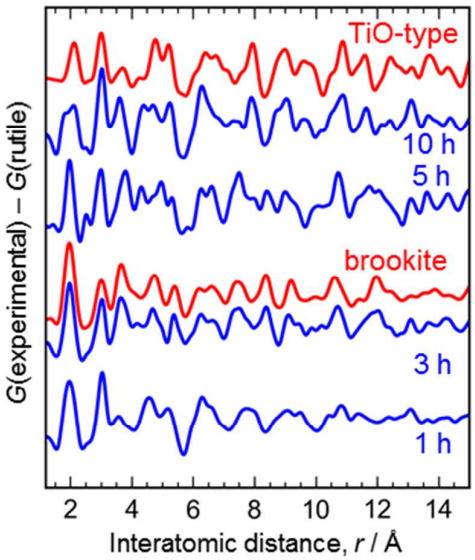

Figure S8. The PDFs showing structure(s) excepting rutile calculated by subtracting rutile PDFs from experimental PDFs: *G*(experimental) – *G*(rutile, fitted) (blue curves) and simulated curves of brookite and TiO-type TiO_2 (red curves). These clarify that lepidocrocite-like structure exists at 1 h, brookite-like structure exist at 3 h, brookite-like structure and TiO-type TiO_2 exist at 5 and 10 h.

8. Additional TEM on the sample annealed for 10 h

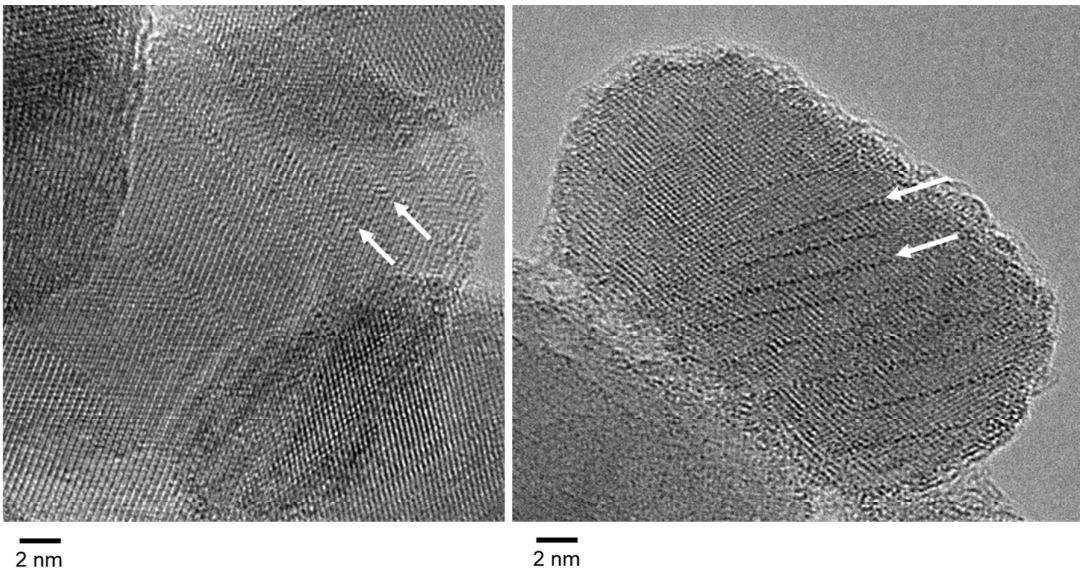

Figure S9. HR-TEM images of large crystals (rutile structure) in the sample annealed for 10 h. The arrows indicate ordered defects (or shear planes).

References

1. Guo, D. H.; Shibuya, R.; Akiba, C.; Saji, S.; Kondo, T.; Nakamura, J., Active sites of nitrogen-doped carbon materials for oxygen reduction reaction clarified using model catalysts. *Science* **2016,** *351* (6271), 361-365.
2. Eland, J. H. D., *Photoelectron Spectroscopy*. Japanese ed.; Japan Scientific Society Publications: Tokyo, 1982.
3. Tominaka, S.; Yoshikawa, H.; Matsushita, Y.; Cheetham, A. K., Topotactic reduction of oxide nanomaterials: unique structure and electronic properties of reduced TiO2 nanoparticles. *Mater Horizons* **2014,** *1* (1), 106-110.
4. Powell, C. J.; Jablonski, A., NIST Standard Reference Database 71: NIST Electron Inelastic-Mean-Free-Path Database: Version 1.2. 2010.